International Journal of Automotive Technology, Vol. 7, No. 1, pp. 9–15 (2006)

1229-9138/2006/025-02

ACTIVATED CARBON CANISTER PERFORMANCE FOR A SPARK IGNITION ENGINE

G. H. CHOI[1)], K. S. CHO[2)], Y. J. CHUNG[2)], J. M. KIM[3)], R. W. DIBBLE[4)] and S. B. HAN[5)*]

[1)]Department of Mechanical & Automotive Engineering, Keimyung University, Daegu 704-701, Korea
[2)]Department of Automotive Engineering, Daegue Mirae College, Daegu 712-716, Korea
[3)]Department of Mechanical Design, Myongji College, Seoul 120-848, Korea
[4)]Department of Mechanical Engineering, University of California at Berkeley, Berkeley, CA 94720, U.S.A.
[5)]Department of Mechanical Engineering, Induk Institute of Technology, Seoul 139-749, Korea

(Received 12 April 2005; Revised 24 September 2005)

ABSTRACT–Prediction of the performance of a carbon canister in vehicle evaporative emission control system has become an important aspect of overall fuel system development and design. A vehicle's evaporative emission control system is continuously working, even when the vehicle is not running, due to generation of vapors from the fuel tank during ambient temperature variations. Evaporative emissions from gasoline powered vehicles continue to be a major concern. The objective of this paper is to clarify the flow characteristics and other such fundamental data for the canister during loading and purging are needed, and this data will prove valuable in the development of the canister. This paper is to evaluate the relationship between carbon canister condition and engine performance during engine operation, and the effects of evaporative emissions on the engine performance were investigated.

KEY WORDS : Evaporative emissions, Canister, Loading, Purge, Purge control solenoid valve, Purge bed volume, HC emissions, CO emissions

1. INTRODUCTION

Automotive exhaust emission regulations are becoming progressively stricter due to increasing awareness of the hazardous effects of exhaust emissions. Improving fuel economy and reducing emissions are two major tasks challenging automotive engineers today. Due to global warming and the limited petroleum resources, automakers are under increasing pressure from the government and public to increase vehicle fuel economy (Yang *et al.*, 2002; Choi *et al.*, 2004).

Evaporative hydrocarbon emissions from gasoline-powered vehicles continue to be a major concern in areas where the national ambient air quality standard for ozone is violated. Evaporative emissions are generally grouped into the following basic categories (Lyons *et al.*, 2000): running losses, hot soak emissions, and diurnal emissions. The latter category is usually divided into two subcategories: resting losses and pressure-driven diurnal emissions.

A vehicle's evaporative emission control system is continuously working, even when the vehicle is not running, due to generation of vapors in the fuel tank during ambient temperature variations (Haskew *et al.*, 1999). Diurnal temperature cycles cause the fuel tank to breathe the fuel vapor in and out, and thus the activated carbon canister is constantly loading and purging the hydrocarbon vapors.

Technologies for reducing evaporative emissions generated from fuel vapor have been developed. To reduce evaporative emissions, both permeation from fuel and vapor lines and breakthrough from the evaporative canister need to be diminished. Fewer fuel line connections are used and hose and valve materials have been modified to reduce permeation (Matsushima *et al.*, 2001).

Lavoie *et al.* (1996) suggested one-dimensional carbon canister adsorption model and has been developed to assist in the prediction of the performance of carbon bed canisters in vehicle evaporative emissions control systems. The model accounts for mass transfer and transient thermal phenomena, both of which are found to be essential in accurately describing canister behavior. The model assumes the vapor above the carbon to be in equilibrium with the adsorbed mass while the local temperature is determined by the dynamic balance between the heat of adsorption, carbon heat capacity and heat loss to ambient.

For the loading and purging of the canister evaporative

*Corresponding author. e-mail: sungbinhan@induk.ac.kr

gas when it is installed on a vehicle, the amount of purge air, loading rate, and other such characteristics must be clarified. In addition, the effects on the engine during loading and purging must be understood so that the canister can be designed to take full advantage of the loading and purging characteristics.

Recently, a fuel vapor system model (Lavoie *et al.*, 1998; Yoo *et al.*, 1999) has been developed to simulate vehicle evaporative emission control system behavior. The fuel system components incorporated into the model include the fuel tank and pump, filler cap, liquid supply and return lines, fuel rail, vent valves, vent line, carbon canister and purge line.

The system is modeled as a vented system of liquid fuel and vapor in equilibrium, subject to a thermal environment characterized by underhood and underbody temperatures and heat transfer parameters assumed known or determined by calibration with experimental liquid temperature data. Numerical calculation (Grieve and Hines, 2000) has allowed canister purge algorithm with a virtual sensor and several studies have reported a carbon canister model.

This paper discusses the relationship between carbon canister condition and engine performance during engine operation, and the effects of evaporative emissions on the engine performance are investigated. The experimental results show the effectiveness of this system for future exhaust emissions and enhanced evaporative emissions. The objective of this paper is to clarify the flow characteristics and other such fundamental data for the canister during loading and purging, and this data will prove valuable in the development of the canister.

2. EXPERIMENTAL SETUP

2.1. View of Canister

Figure 1 shows the experimental canister, and Figure 2 shows the cross-sectional view of the canister. There are three openings to the canister: Inlet for the evaporation gas to enter from the fuel tank, exit leading to the intake port of the engine, and a purge port for the clean, external air. On the top and bottom sections of the cylindrical canister have 3 mm thick filters and a grid, and there are air gaps between the filters and the ports. The interior of the canister is filled with activated carbons.

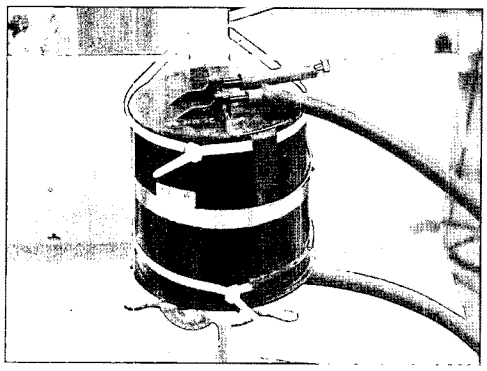

Figure 1. Experimental canister.

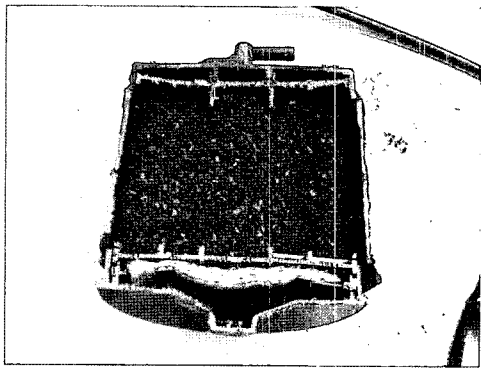

Figure 2. Cross-sectional view of the canister.

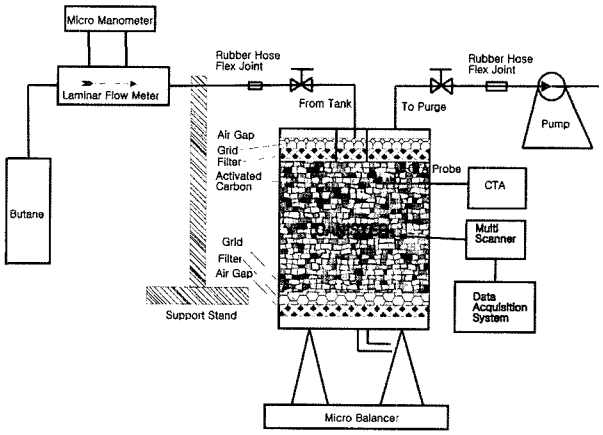

Figure 3. Schematic diagram of experimental apparatus.

2.2. Experimental Apparatus

To clarify the temperature distribution characteristics within the canister at loading and purging, a total of 30 T type thermocouples were installed (see Figure 3). Temperature measurements were taken at 10 second intervals using Multiscan/1200 from IOtech, and data were acquired using Chartview. Pressure loss was measured with a pressure gauge located at each port.

In order to understand the flow characteristics of the evaporation gas within the canister, a flow characteristic testing apparatus was constructed as shown in Figure 4.

Figure 5 shows the schematic diagram of the experimental apparatus. The engine speed was increased from 850 rpm to 2500 rpm. To clarify the canister characteristics, engine speed variations, stability, CO, and HC emissions were measured when the hydrocarbon flowed into the canister.

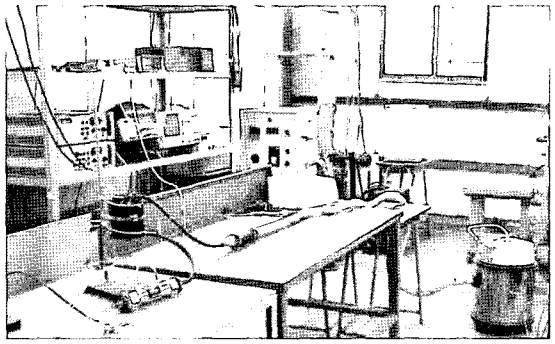

Figure 4. Flow characteristics testing apparatus.

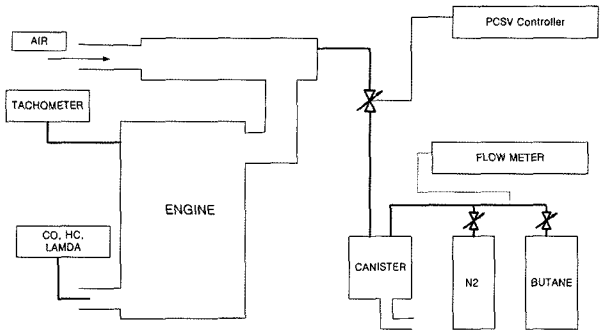

Figure 5. Schematic diagram of the experimental apparatus.

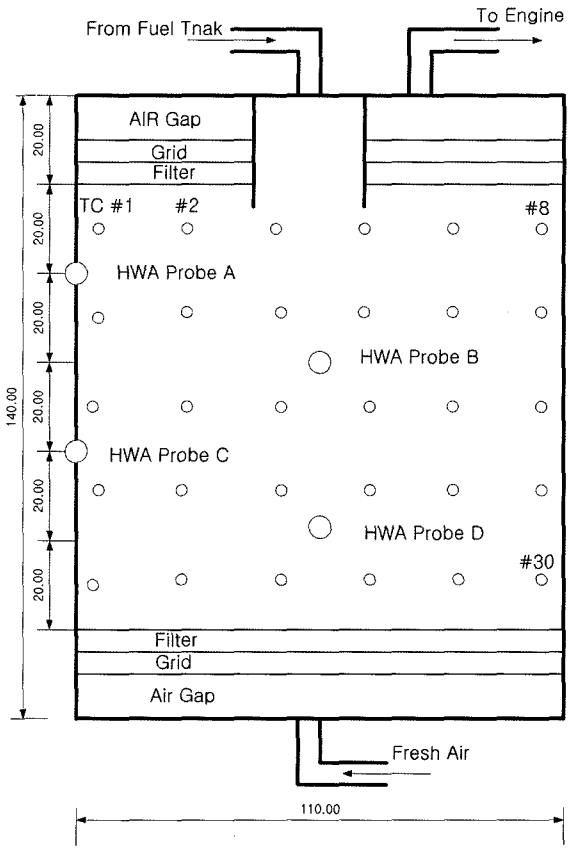

Figure 6. Schematic diagram of the canister and the measurement locations.

A vacuum pump was used to inject and extract air to simulate loading and purge conditions. The flow rate of this air was measured using a laminar flow meter, and the velocity distribution within the canister was measured using a constant temperature anemometer. Temperature was measured using a platinum hot wire probe with a diameter of 5 μm, and the measurement locations were 20 mm and 60 mm from the top and 40 mm and 80 mm in the vertical direction, for a total of four locations at 10 mm depth increments measuring the velocity in the radial direction (see Figure 6).

For the loading and purging of the canister fuel vapor when it is installed on a vehicle, it must be clarified. In addition, the effects on the engine during loading and purging must be understood so that the canister can be designed to take full advantage of the loading and purging characteristics. The engine used in this experiment was Hyundai Motor Company's Sonata 1.8 DOHC. To control the hydrocarbon concentration that flows in afterwards, the amount of nitrogen was the adjusted proportion. The experiments were performed in three steps at nitrogen versus hydrocarbon per volume proportions 100/0, 75/25, and 50/50.

During loading, the vacuum pump was connected to the fresh air part of the canister with the purge valve closed, and flow was controlled using the inlet valve and measured using a laminar flow meter. During purging, the location of the vacuum pump was switched, and the air was purged at the same flow rate. Loading was performed in four steps at 0.3 *l*, 0.6 *l*, 0.9 *l*, and 3 *l* per minute while purging was done in four steps at 6.0 *l*, 7.8 *l*, 15.0 *l*, and 21.0 *l* per minute.

3. RESULTS AND DISCUSSION

3.1. Loading Characteristics

Figure 7 shows the hydrocarbon volume at different loading rates. In this figure, the inflow of gas into the canister is increasing proportionally to time. Since the amount of loading gradually increases as loading rate is decreased, the loading rate should be minimized to allow for absorption.

When the loading rate is increased, the temperature of the canister increases significantly due to heat generated during loading. The temperature reaches 80°C at times, and has an adverse effect on absorption. As the volume of hydrocarbons increase, the weight of the gas also the gas also increases gradually. When the loading rate is 3.0 *l*/ min, 75 g is absorbed, and when the loading rate is 0.3 *l*/

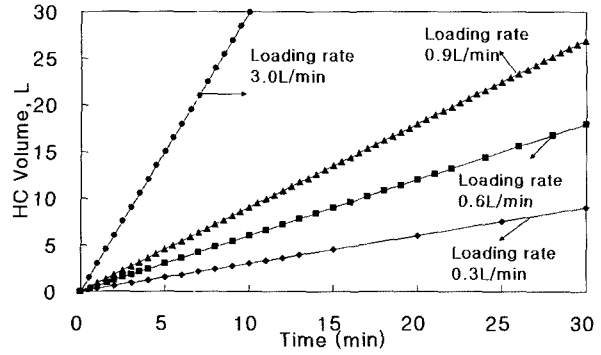

Figure 7. Hydrocarbon volume vs. time at different loading rates.

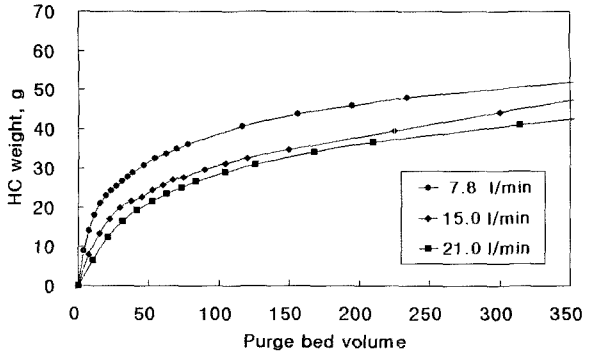

Figure 9. Relationship between purge bed volume and hydrocarbon weight for purge rates.

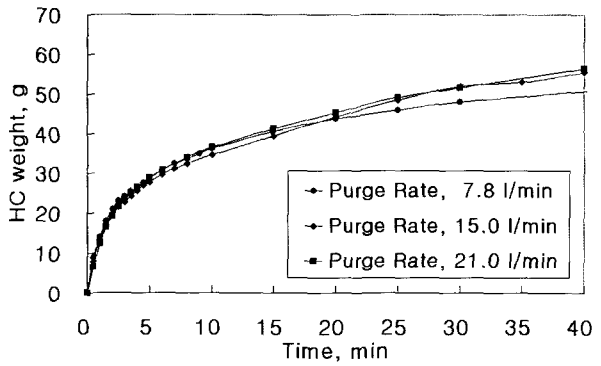

Figure 8. Relationship between time and hydrocarbon weight at different purge rates.

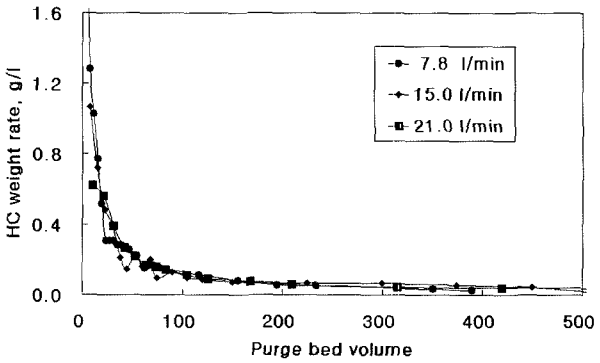

Figure 10. Relationship between purge bed volume and hydrocarbon weight rate for purge rates.

min, up to 150 g is absorbed.

3.2. Purge Characteristics

Figure 8 shows the time dependence of the HC weight at different purge rates. A large amount of hydrocarbon is purged initially and slowly increases as time goes on. The amount of hydrocarbons purged increases with the purge rate, but the change is very small. The volume of hydrocarbons that is desorbed is dependent on time. Generally, the total amount of air that passes through the activated carbon bed is the product of the purge rate and purge time, and this is defined as the purge bed volume.

Figure 9 shows the weight of the hydrocarbon as a function of the purge bed volume at different purge rates. The amount of hydrocarbons that is desorbed increases as the purge bed volume increases. When the purge bed volume is small, the amount of hydrocarbons that is desorbed increases abruptly, and after a certain bed volume, the amount desorbed gradually increases. Namely, a large amount exits upon desorption early during purging, and since the amount purged continues to decrease, it is well known that a large amount of hydrocarbons will be desorbed in an actual engine during the early stage of a PCSV (Purge Control Solenoid Valve)'s opening.

Figure 10 shows the weight of the HC in the purged vapor as a function of the purge bed volume. The weight of the HC is large when the purge bed volume is small, but it decreases rapidly as the purge bed volume increases. This shows that, in the early stages of an PCSV's operation, highly concentrated gas flows into the engine, whereas a dilute gas flows in afterwards.

Since it is more likely for the engine to be in a bad condition in the latter stage than in the early stage, canister and the engine must be taken into consideration in the designing operation time setup mode of the PCSV.

3.3. Temperature Characteristics

Figures 11 and 12 show the temperature difference during absorption and desorption as a function of time at varying canister locations. It can be seen that heat generated during loading initially causes a significant temperature increase but later decreases gradually.

Upon desorption, the reverse process of heat absorption is shown. Distribution during absorption and desorption shows that the hydrocarbons are absorbed desorbed

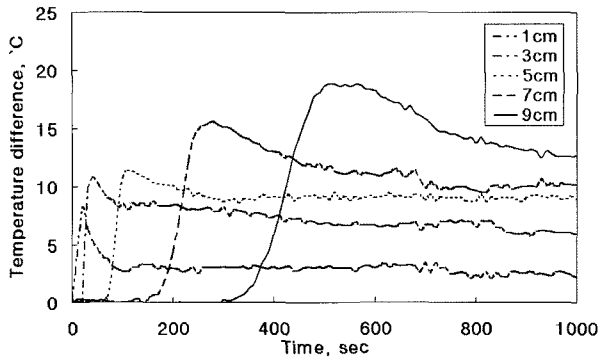

Figure 11. Temperature difference vs. time during loading.

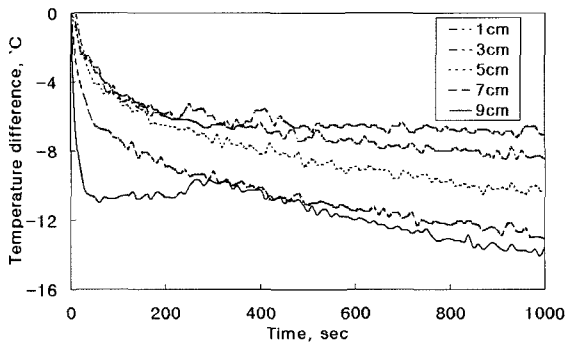

Figure 12. Temperature difference vs. time during purging.

gradually from the port entrance towards the center and becomes symmetric as time passes, showing a distribution with no dead zone.

The amount of gas that is loaded increases as the loading rate is decreased and the time increased, and the purging improves as the purge rate is increased. The hydrocarbons that are purged initially have a high concentration, and a large amount is purged. During loading and purging, the temperature initially increases and decreases drastically due to heat generation and heat loss.

3.4. Engine Characteristics

Figure 13 shows the engine speed increase ratio when the volume rate of hydrocarbon versus nitrogen that flow into engine are 0%, 25%, and 50%. As the volume rate of hydrocarbon increases, the engine speed increases remarkably. In particular, the engine speed increase at around idling of 850 rpm appears larger. The reason of the increase in engine speed could be that supplement supply of fuel vapor through inlet system at around idling engine speed make the mixture rich. Since the inflow of air into the canister increases as the engine speed is increased, the effect of supplement supply of fuel vapor seems relatively small.

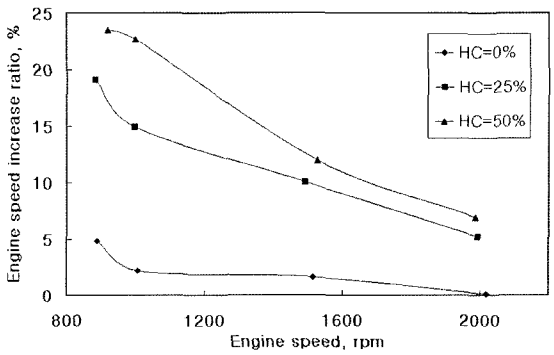

Figure 13. Engine speed increase ratio vs. engine speed.

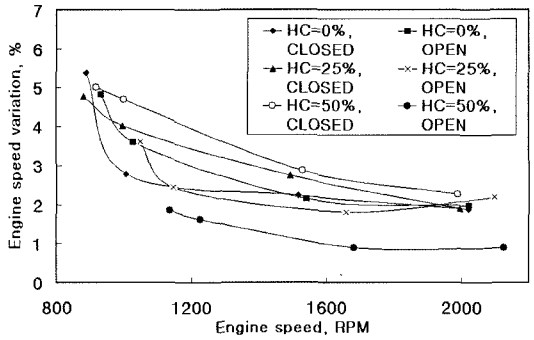

Figure 14. Engine speed variation vs. engine speed.

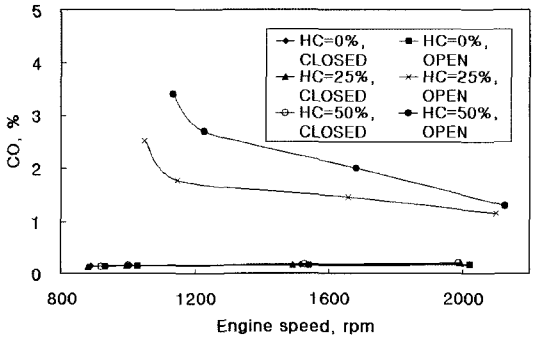

Figure 15. Carbon monoxide vs. engine speed.

Figure 14 shows engine speed variation as a function of inflow of hydrocarbon. The engine speed variation is defined as the half of difference between maximum engine speed and minimum engine speed during a specified period into mean engine speed. In case of 0% hydrocarbon, engine speed variation increases a small quantity, but the engine speed variation decreases in 25% hydrocarbon and 50% hydrocarbon. Since the engine speed increases as the supply of hydrocarbon is increased, the engine speed variation is getting smaller and the stability will improve.

In Figure 15, CO emissions versus engine speed is

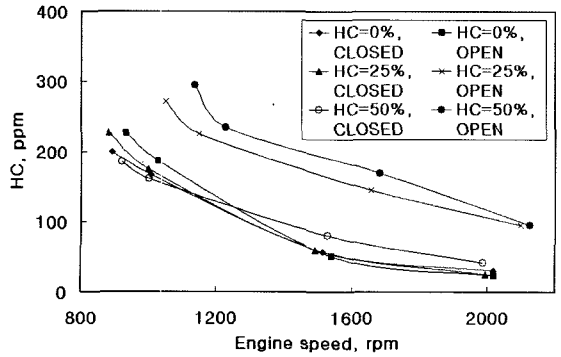

Figure 16. Hydrocarbon emissions vs. engine speed.

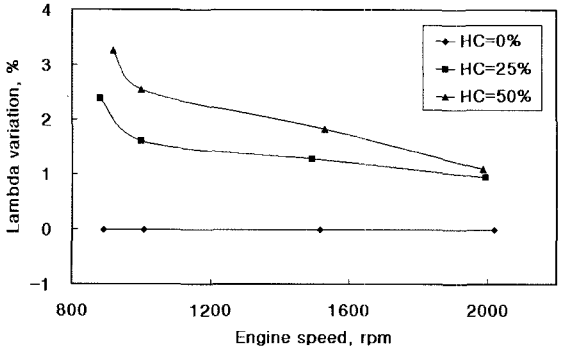

Figure 18. Lambda variation vs. engine speed.

plotted. The exhaust gas emissions (CO, CO_2, THC, O_2, NOx) were measured in this research project by a Horiba gas analyzer (Mexa 9100DEGR).

It shows the trends of CO emissions according to the hydrocarbon supply during the engine operation. CO emissions shown in the figure are high since hydrocarbon increases according to opening the purge control solenoid valve (PCSV), and CO emissions are high as engine speed is low. The reason for the increase in CO emissions could be the lack of oxygen increase with the increase of fuel gas supplement in inlet system which results in the imperfect combustion.

Figure 16 shows the trends of hydrocarbon emissions according to the hydrocarbon supply during the engine operation. The inflow of evaporative emissions makes the engine speed high and the speed variation low, but CO emissions and HC emissions increase. In particular, accurate control for inflow of fuel vapor at idling is required.

In Figure 17, is a plot of the lambda results. When the PCSV is open in 0% hydrocarbon, air-fuel ratio shows lean. But it shows that the lambda shows rich according to 25% or 50% hydrocarbon. The trends increase as rate of hydrocarbon increases and engine speed is low.

Figure 18 shows lambda variation according to the hydrocarbon vapor supply. The lambda variation is the

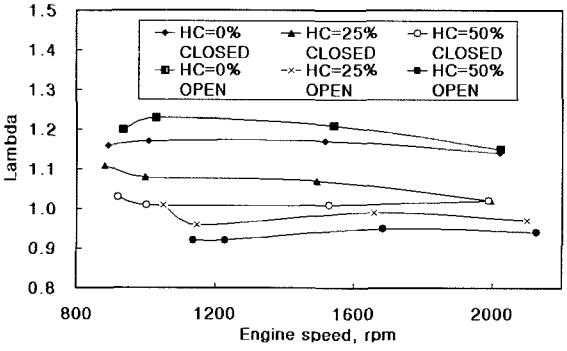

Figure 17. Lambda vs. engine speed.

standard deviation in power of zirconia O_2 sensor divided by the mean power of sensor (power voltage range: 0~1 V). It can be seen that lambda variation without supplementary hydrocarbon supply is continuously zero but lambda variation increases greatly at 25% or 50% hydrocarbon. The lambda variation seems to be large in low engine speed or idling, and small as engine speed is increased.

4. CONCLUSIONS

This study is to clarify the activated carbon canister performance for a spark ignition engine. The results obtained are as follows.

Since the engine speed increases as the supply of hydrocarbon is increased, the engine speed variation is getting smaller and the stability can be increased. CO emissions are high since hydrocarbon increases according to opening the PCSV, and CO emissions are high as engine speed is low. The inflow of evaporative emissions makes the engine speed high and the speed variation low, but CO emissions and HC emissions increase. In particular, accurate control for inflow of fuel vapor at idling is required.

The lambda variation seems to be large in low engine speed or idling, and small as engine speed is increased. The measurements taken for HC emissions and the lambda in the exhaust manifold show that the PCSV controller and the design of the canister affect mixture and engine's HC emissions.

ACKNOWLEDGEMENTS-This work was supported by grant No. RTI04-03-02 from the Regional Technology Innovation Program of the Ministry of Commerce, Industry and Energy (MOCIE).

REFERENCES

Choi, G. H., Han, S. B. and Dibble, R. W. (2004). Experimental study on homogeneous charge compression ignition engine operation with exhaust gas

recirculation. *Int. J. Automotive Technology* **5**, **3**, 195–200.

Grieve, M. J. and Himes, E. G. (2000). Advanced canister purge algorithm with a virtual HC sensor. *SAE Paper No.* 2000-01-0557.

Haskew, H. M. and Liberty, T. F. (1999). Diurnal emissions from in-use vehicle. *SAE Paper No.* 1999-01-1463.

Haskew, H. M., Eng, K. D. and Liberty, T. F. (1999). Running loss emission from in-use vehicle. *SAE Paper No.* 1999-01-1464.

Lavoie, G. A., Johnson, P. J. and Hood, J. F. (1996). Carbon canister modeling for evaporative emission: Adsorption and thermal effects. *SAE Paper No.* 961210.

Lyons, J. M., Lee, J. M., Heirigs, P. L., McClement, D. and Welstand, S. (2000). Evaporative emissions from late-model in-use vehicles. *SAE Paper No.* 2000-01-2958.

Matsushima, H., Iwamoto, A., Ogawa, M., Satoh, T. and Ozaki, K. (2001). Development of a gasoline-fueled vehicle with zero evaporative emissions. *SAE Paper No.* 2001-01-2926.

Yang, J., Culp, T. and Kenney, T. (2002). Development of a gasoline engine system using HCCI technology - the concept and the test results. *SAE Paper No.* 2002-01-2832.

Yoo, I. K., Upadhyay, D. and Rizzoni, G. (1999). A control-oriented carbon canister model. *SAE Paper No.* 1999-01-1103.